Crystal structure of tramadol hydrochloride, $C_{16}H_{26}NO_2Cl$

James A. Kaduk,[1,a] Kai Zhong,[2] Amy M. Gindhart,[2] and Thomas N. Blanton[2]
[1]*Illinois Institute of Technology, 3101 S. Dearborn Street, Chicago, Illinois 60616*
[2]*ICDD, 12 Campus Blvd., Newtown Square, Pennsylvania, 19073-3273*

(Received 10 March 2015; accepted 26 April 2015)

The crystal structure of tramadol hydrochloride has been solved and refined using synchrotron X-ray powder diffraction data, and optimized using density functional techniques. Tramadol hydrochloride crystallizes in space group *Cc* (#9) with $a = 9.680\,72(2)$, $b = 19.191\,27(4)$, $c = 9.285\,94(1)$ Å, $\beta = 100.5923(1)°$, $V = 1695.795(5)$ Å^3, and $Z = 4$. The solid-state conformation of the cation differs from the minimum-energy conformation of the tramadol cation in water, and from the conformation observed in the benzoic acid adduct of tramadol hydrochloride. N–H···Cl and O–H···Cl hydrogen bonds form a zigzag chain with graph set *C*1,2(8) along the *c*-axis. C–H···O hydrogen bonds also contribute to the crystal energy. The powder pattern has been submitted to ICDD for inclusion in the Powder Diffraction File™. © *2015 International Centre for Diffraction Data.*
[doi:10.1017/S088571561500041X]

Key words: tramadol hydrochloride, Ultram, powder diffraction, Rietveld refinement, density functional theory

I. INTRODUCTION

Tramadol (marketed as Ultram) is an opioid centrally acting binary analgesic drug, used to treat moderate to moderately severe pain. The systematic name (CAS Registry Number 36282-47-0) of tramadol is 2-[(dimethylamino)methyl]-1-(3-methoxyphenyl)cyclohexanol. With two chiral centers, tramadol may exist in four different isomer forms. Marketed tramadol is the hydrochloride form of (1R, 2R)-(+)isomer and (1S, 2S)-(−)isomer racemic mixtures. The (+)isomer is a selective agonist of μ receptors, and (−)isomer functions primarily to inhibit noradrenaline reuptake. The two enantiomers complement each other's analgesic activity (Brayfield, 2013). Recently Bag and Reddy (2014) reported the solved crystal structure of tramadol hydrochloride from single-crystal diffraction data. A two-dimensional (2D) molecular diagram is shown in Figure 1.

The presence of high-quality reference powder patterns in the PDF® (Powder Diffraction File; ICDD, 2014) is important for phase identification, particularly by pharmaceutical, forensic, and law enforcement scientists. The crystal structures of a significant fraction of the largest dollar volume pharmaceuticals have not been published, and thus calculated powder patterns are not present in the PDF-4 databases. Sometimes experimental patterns are reported, but they are generally of low quality. This structure is a result of a collaboration among ICDD, Illinois Institute of Technology (IIT), Poly Crystallography Inc., and Argonne National Laboratory to measure high-quality synchrotron powder patterns of commercial pharmaceutical ingredients, include these reference patterns in the PDF, and determine the crystal structures of these active pharmaceutical ingredients (APIs).

Even when the crystal structure of an API is reported, the single-crystal structure was often determined at low temperature. Most powder measurements are performed at ambient conditions. Thermal expansion (often anisotropic) means that the peak positions calculated from a low-temperature single-crystal structure often differ significantly from those measured at ambient conditions. These peak shifts can result in failure of default search/match algorithms to identify a phase, even when it is present in the sample. High-quality reference patterns measured at ambient conditions are thus critical for easy identification of APIs using standard powder diffraction practices.

II. EXPERIMENTAL

Tramadol hydrochloride, a commercial reagent, purchased from the United States Pharmacopeia (USP) (lot G0L065), was used as-received. The white powder was packed into a 1.5 mm diameter Kapton capillary, and rotated during the measurement at ~50 cycles s^{-1}. The powder

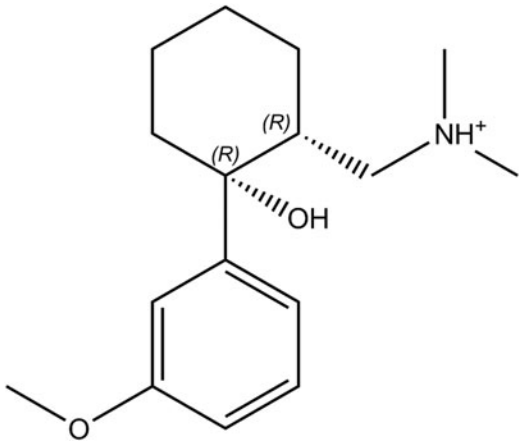


Figure 1. The molecular structure of the (1R,2R) tramadol cation.

[a]Author to whom correspondence should be addressed. Electronic mail: kaduk@polycrystallography.com

https://doi.org/10.1017/S088571561500041X Published online by Cambridge University Press

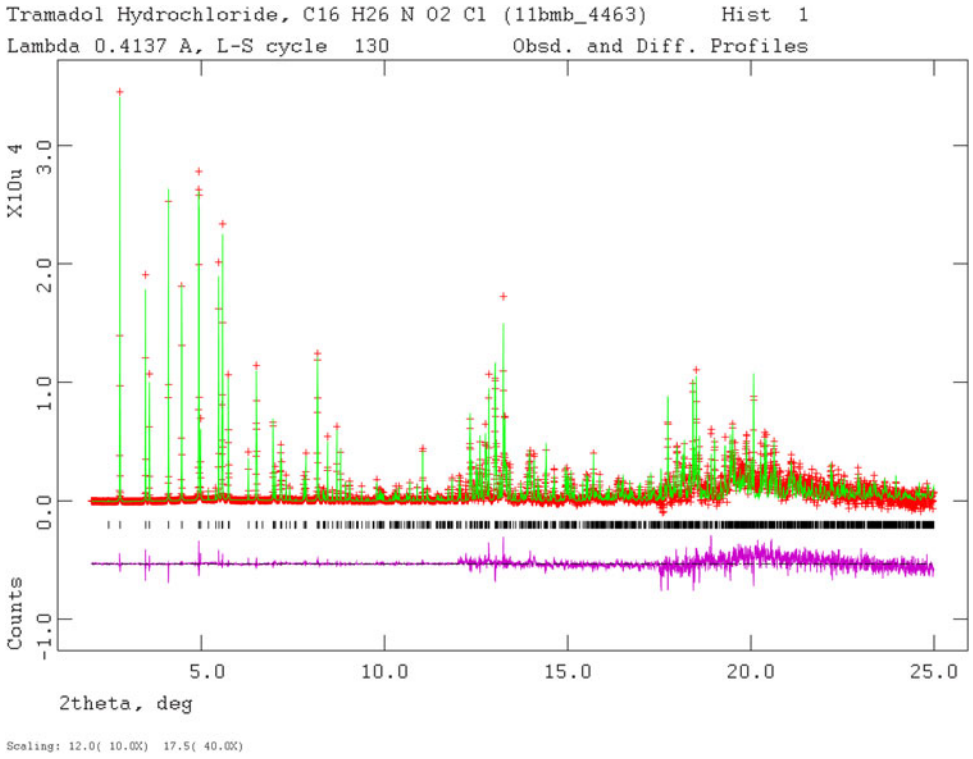


Figure 2. (Color online) The Rietveld plot for the refinement of tramadol hydrochloride. The red crosses represent the observed data points, and the green line is the calculated pattern. The magenta curve is the difference pattern, plotted at the same vertical scale as the other patterns. The vertical scale has been multiplied by a factor of 10 for $2\theta > 12.0°$ and by a factor of 40 for $2\theta > 17.5°$.

TABLE I. Rietveld refined crystal structure of tramadol hydrochloride.

Crystal data	
$C_{16}H_{26}ClNO_2$	$\beta = 100.5923\ (1)°$
$M_w = 299.84$	$V = 1695.795\ (5)$ Å^3
Monoclinic, *Cc*	$Z = 4$
$a = 9.680\ 72\ (2)$ Å	Synchrotron radiation, $\lambda = 0.413\ 685$ Å
$b = 19.191\ 27\ (4)$ Å	$T = 295$ K
$c = 9.285\ 94\ (1)$ Å	Cylinder, 1.5×1.5 mm^2
Data collection	
11-BM APS diffractometer	Scan method: step
Specimen mounting: Kapton capillary	$2\theta_{min} = 0.5°$, $2\theta_{max} = 50.0°$, $2\theta_{step} = 0.001°$
Data collection mode: transmission	
Refinement	
Least-squares matrix: full	49496 data points
$R_p = 0.057$	Profile function: CW Profile function number 4 with 21 terms Pseudovoigt profile coefficients as parameterized in Thompson *et al.* (1987). Asymmetry correction of Finger *et al.* (1994). Microstrain broadening by Stephens (1999). #1(GU) = 3.200 #2(GV) = −0.126 #3(GW) = 0.063 #4(GP) = 0.000 #5(LX) = 0.173 #6(ptec) = 0.00 #7(trns) = 0.00 #8(shft) = 0.0000 #9 (sfec) = 0.00 #10(S/L) = 0.0011 #11(H/L) = 0.0011 #12(eta) = 0.6048 #13(S400) = 5.6×10^{-3} #14(S040) = 2.8×10^{-4} #15(S004) = 2.4×10^{-3} #16(S220) = 2.7×10^{-3} #17(S202) = -9.8×10^{-4} #18(S022) = 1.2×10^{-3} #19(S301) = 6.2×10^{-5} #20(S103) = 5.0×10^{-4} #21(S121) = -5.0×10^{-4} Peak tails are ignored where the intensity is below 0.0010 times the peak Aniso. broadening axis 0.0 0.0 1.0
$R_{wp} = 0.070$	83 parameters
$R_{exp} = 0.048$	36 restraints
$R(F^2) = 0.131\ 76$	$(\Delta/\sigma)_{max} = 0.07$
$\chi^2 = 2.220$	Background function: GSAS Background function number 1 with three terms. Shifted Chebyshev function of first kind 1: 212.624 2: 0.655 652 3: −6.231 37

Continued

https://doi.org/10.1017/S088571561500041X Published online by Cambridge University Press

TABLE I. Continued

Fractional atomic coordinates and isotropic or equivalent isotropic displacement parameters (Å²)

	x	*y*	*z*	U_{iso}*/U_{eq}
C1	0.8086 (2)	0.402 66 (15)	0.5905 (3)	0.0456 (7)*
C2	0.8689 (3)	0.364 22 (13)	0.7131 (3)	0.0456 (7)*
C3	1.0087 (3)	0.375 30 (14)	0.7776 (3)	0.0456 (7)*
C4	1.0882 (3)	0.424 82 (15)	0.7195 (3)	0.0456 (7)*
C5	1.0280 (3)	0.464 31 (13)	0.5947 (3)	0.0456 (7)*
C6	0.8880 (3)	0.452 18 (14)	0.5324 (3)	0.0456 (7)*
H7	0.8142 (4)	0.330 07 (16)	0.7531 (4)	0.0593 (10)*
H8	1.1986 (3)	0.4336 (2)	0.7705 (5)	0.0593 (10)*
H9	1.0825 (4)	0.497 41 (17)	0.5568 (4)	0.0593 (10)*
H10	0.8463 (4)	0.478 69 (19)	0.4478 (3)	0.0593 (10)*
O11	1.0478 (4)	0.336 62 (17)	0.9020 (4)	0.0711 (10)*
C12	1.1864 (5)	0.3495 (2)	0.9850 (5)	0.0711 (10)*
O13	0.6015 (3)	0.329 19 (14)	0.5765 (3)	0.0293 (5)*
C14	0.6521 (3)	0.391 89 (15)	0.5212 (4)	0.0293 (5)*
C15	0.6280 (4)	0.380 80 (18)	0.3517 (4)	0.0293 (5)*
C16	0.4693 (4)	0.3760 (2)	0.2890 (4)	0.0293 (5)*
C17	0.3874 (4)	0.4398 (2)	0.3249 (4)	0.0293 (5)*
C18	0.4129 (4)	0.4487 (2)	0.4914 (4)	0.0293 (5)*
C19	0.5670 (4)	0.455 41 (19)	0.5571 (4)	0.0293 (5)*
C20	0.7078 (5)	0.3149 (2)	0.3170 (4)	0.0762 (11)*
N21	0.7494 (4)	0.315 67 (17)	0.1676 (4)	0.0762 (11)*
C22	0.7739 (6)	0.2447 (2)	0.1167 (5)	0.0762 (11)*
C23	0.8682 (5)	0.3641 (2)	0.1616 (5)	0.0762 (11)*
H24	1.254 43	0.367 82	0.910 36	0.0924 (14)*
H25	1.2296	0.3051	1.037 06	0.0924 (14)*
H26	1.175 22	0.391 23	1.065 54	0.0924 (14)*
H27	0.583 63	0.3377	0.666 86	0.0381 (7)*
H28	0.677 15	0.420 01	0.301 19	0.0381 (7)*
H29	0.453 67	0.3754	0.164 76	0.0381 (7)*
H30	0.417	0.334 74	0.325	0.0381 (7)*
H31	0.4386	0.490 84	0.277 27	0.0381 (7)*
H32	0.281 33	0.443 58	0.279 36	0.0381 (7)*
H33	0.371 32	0.409 49	0.534 61	0.0381 (7)*
H34	0.364 92	0.499 34	0.5201	0.0381 (7)*
H35	0.585 73	0.464 49	0.6766	0.0381 (7)*
H36	0.617 34	0.502 88	0.514 76	0.0381 (7)*
H37	0.795 18	0.303 05	0.396 55	0.0991 (14)*
H38	0.630 63	0.265 65	0.322 53	0.0991 (14)*
H39	0.721 83	0.201 17	0.162 13	0.0991 (14)*
H40	0.892 01	0.233 28	0.155 46	0.0991 (14)*
H41	0.756 33	0.240 61	0.000 32	0.0991 (14)*
H42	0.9425	0.335 21	0.128 52	0.0991 (14)*
H43	0.872 33	0.391 72	0.251 48	0.0991 (14)*
H44	0.809 33	0.3959	0.061 47	0.0991 (14)*
H45	0.652 02	0.325 58	0.090 89	0.0991 (14)*
Cl46	0.039 57	0.149 38 (8)	0.3943	0.078 97

Atomic displacement parameters (Å²)

	U^{11}	U^{22}	U^{33}	U^{12}	U^{13}	U^{23}
Cl46	0.0626 (13)	0.140 (2)	0.0329 (10)	−0.0066 (15)	0.0056 (9)	−0.0028 (15)

pattern was measured at 295 K at beamline 11-BM (Lee *et al.*, 2008; Wang *et al.*, 2008) of the Advanced Photon Source at Argonne National Laboratory using a wavelength of 0.413 685 Å from 0.5 to 50°2θ with a step size of 0.001° and a counting time of 0.1 s step^{-1}. The pattern was indexed on a primitive monoclinic unit cell having $a = 9.678$, $b = 19.187$, $c = 9.284$ Å, $\beta = 100.6°$, $V = 1694.6$ Å^3, and $Z = 4$ using Jade 9.5 (MDI, 2014), which suggested the space group *Cc*. Since the commercial material is a racemate, the space group is reasonable, and was confirmed by successful solution and refinement of the structure. A reduced cell search in the Cambridge Structural Database (Allen, 2002) yielded 638 hits; combining it with the chemistry "C H N O Cl only" yielded 18 hits, but no structure for tramadol hydrochloride. A name search on "tramadol" yielded 3 hits. Two of these were other salts, but one was the benzoic acid adduct of tramadol hydrochloride (AYUNUE; Siddaraju *et al.*, 2011). A connectivity search in the CSD yielded the structure of

https://doi.org/10.1017/S088571561500041X Published online by Cambridge University Press

TABLE II. DFT-optimized (CRYSTAL09) crystal structure of tramadol hydrochloride.

Crystal data	
$C_{16}H_{26}NO_2Cl$	$\beta = 100.5923°$
$M_w = 299.84$	$V = 1695.80$ Å^3
Monoclinic, *Cc*	$Z = 4$
$a = 9.6807$ Å	
$b = 19.1913$ Å	
$c = 9.2859$ Å	

Fractional atomic coordinates and isotropic displacement parameters(Å^2)

	x	*y*	*z*	U_{iso}
C1	0.303 35	−0.097 99	0.585 74	0.045 60
C2	0.362 65	−0.138 73	0.705 21	0.045 60
C3	0.501 74	−0.128 82	0.776 70	0.045 60
C4	0.586 20	−0.078 69	0.726 25	0.045 60
C5	0.527 00	−0.038 46	0.604 70	0.045 60
C6	0.387 51	−0.046 88	0.535 67	0.045 60
H7	0.300 72	−0.178 73	0.745 38	0.059 30
H8	0.649 99	−0.071 47	0.778 11	0.059 30
H9	0.592 09	0.000 22	0.564 10	0.059 30
H10	0.345 18	−0.013 13	0.444 28	0.059 30
O11	0.543 98	−0.171 63	0.894 11	0.071 10
C12	0.678 12	−0.160 14	0.985 41	0.071 10
O13	0.094 90	−0.170 70	0.571 28	0.029 30
C14	0.147 79	−0.108 60	0.516 78	0.029 30
C15	0.126 03	−0.118 71	0.347 90	0.029 30
C16	−0.031 92	−0.124 52	0.281 55	0.029 30
C17	−0.115 72	−0.061 83	0.321 40	0.029 30
C18	−0.094 55	−0.051 89	0.487 44	0.029 30
C19	0.062 22	−0.044 75	0.552 18	0.029 30
C20	0.207 00	−0.183 16	0.311 30	0.076 20
N21	0.254 31	−0.179 73	0.165 43	0.076 20
C22	0.296 45	−0.250 46	0.121 02	0.076 20
C23	0.369 60	−0.128 43	0.164 19	0.076 20
H24	0.763 97	−0.161 15	0.923 70	0.092 40
H25	0.691 05	−0.202 90	1.063 96	0.092 40
H26	0.680 32	−0.109 96	1.042 12	0.092 40
H27	0.079 83	−0.162 33	0.671 41	0.092 40
H28	0.167 22	−0.071 86	0.303 12	0.092 40
H29	−0.044 70	−0.130 02	0.162 46	0.092 40
H30	−0.071 11	−0.172 32	0.32 461	0.092 40
H31	−0.080 46	−0.014 39	0.273 12	0.092 40
H32	−0.227 62	−0.068 16	0.274 73	0.092 40
H33	−0.137 80	−0.096 57	0.537 76	0.092 40
H34	−0.150 65	−0.005 49	0.514 10	0.09 240
H35	0.078 47	−0.039 45	0.671 47	0.092 40
H36	0.102 85	0.002 45	0.508 05	0.092 40
H37	0.302 11	−0.192 22	0.392 76	0.099 10
H38	0.140 88	−0.229 27	0.308 24	0.099 10
H39	0.203 40	−0.283 58	0.102 44	0.099 10
H40	0.375 51	−0.272 21	0.208 34	0.099 10
H41	0.338 48	−0.245 71	0.020 53	0.099 10
H42	0.401 39	−0.130 84	0.057 86	0.099 10
H43	0.457 95	−0.142 25	0.250 35	0.099 10
H44	0.333 36	−0.076 15	0.182 61	0.099 10
H45	0.169 52	−0.165 11	0.083 15	0.099 10
Cl46	0.031 59	−0.148 95	−0.108 48	0.078 60

the acrylonitrile solvate of tramadol hydrochloride (VISQAR; Boumendjel *et al.*, 2013).

A (1R,2R)-tramadol cation was built and its conformation optimized using Spartan '14 (Wavefunction, 2013), and saved as a mol2 file. This file was converted into a Fenske–Hall *Z*-matrix file using OpenBabel (O'Boyle *et al.*, 2011). This fragment and a Cl atom were used to solve the structure with FOX (Favre-Nicolin and Černý, 2002). The maximum $\sin\theta/\lambda$ used in the solution was 0.40 Å^{-1}.

Rietveld refinement was carried out using GSAS (Larson and Von Dreele, 2004). Only the 2.0–25.0° portion of the pattern was included in the refinement ($d_{min} = 0.95$ Å). All non-H

https://doi.org/10.1017/S088571561500041X Published online by Cambridge University Press

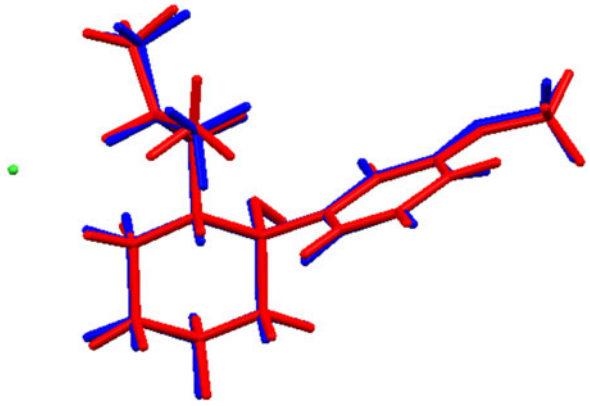


Figure 3. (Color online) Comparison of the refined and optimized structures of tramadol hydrochloride. The Rietveld refined structure is in red, and the DFT-optimized structure is in blue.

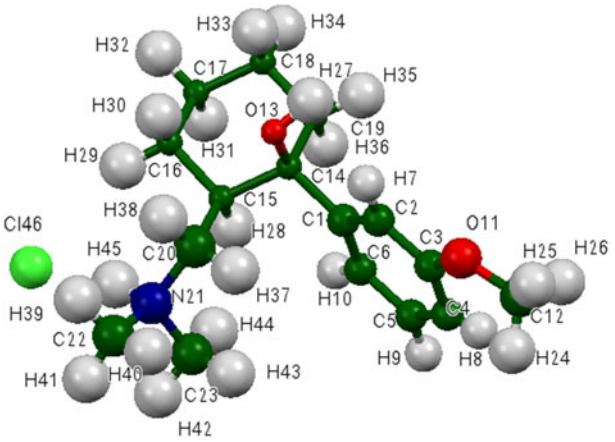


Figure 4. (Color online) The molecular structure of tramadol hydrochloride, with the atom numbering. The atoms are represented by 50% probability spheroids.

bond distances and angles were subjected to restraints, based on a Mercury/Mogul Geometry Check (Bruno *et al.*, 2004; Sykes *et al.*, 2011) of the molecule. The Mogul average and standard deviation for each quantity were used as the restraint parameters. The restraints contributed 1.94% to the final χ^2. Isotropic displacement coefficients were refined, grouped by chemical similarity, and the Cl was refined anisotropically. The hydrogen atoms were included in calculated positions, which were recalculated during the refinement. The U_{iso} of each hydrogen atom was constrained to be 1.3× that of the heavy atom to which it is attached. The peak profiles were described using profile function #4 (Thompson *et al.*, 1987; Finger *et al.*, 1994), which includes the Stephens (1999) anisotropic strain broadening model. The background was modeled using a three-term shifted Chebyshev polynomial, with a five-term diffuse scattering function to model the Kapton capillary and any amorphous component. The final refinement of 83 variables using 23 038 observations (23002 data points and 36 restraints) yielded the residuals $R_{wp} = 0.070$, $R_p = 0.057$, and $\chi^2 = 2.234$. The largest peak (1.55 Å from C6) and hole (3.06 Å from O13) in the difference Fourier map were 0.53 and -0.43 eÅ^{-3}, respectively. The Rietveld plot is included as Figure 2. The largest errors are in the shapes of the

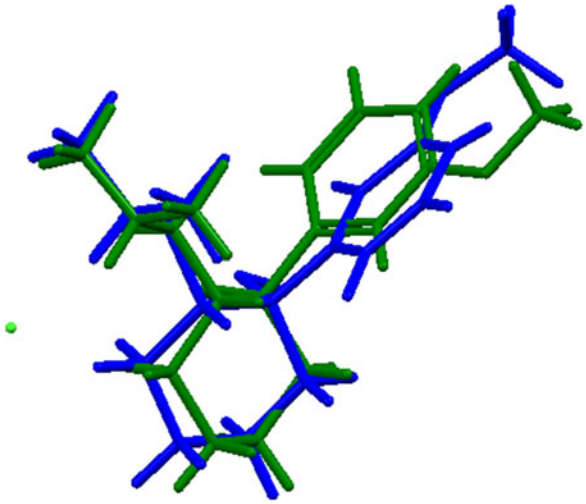


Figure 6. (Color online) Comparison of the tramadol cations in the hydrochloride (this structure; blue) and tramadol hydrochloride benzoic acid adduct (AYUNUE; green).

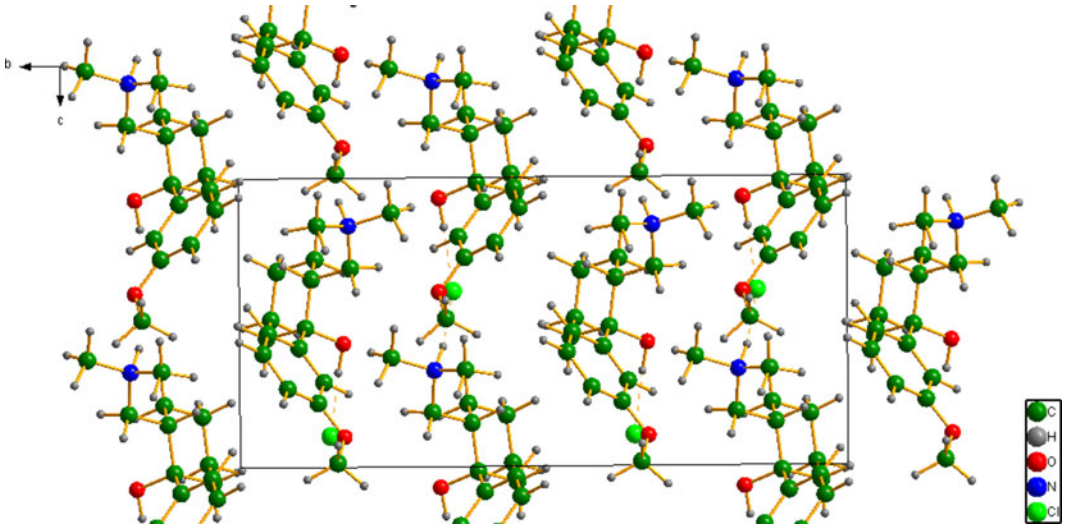


Figure 5. (Color online) The crystal structure of tramadol hydrochloride, viewed down the *a*-axis. The hydrogen bonds are shown as dashed lines.

https://doi.org/10.1017/S088571561500041X Published online by Cambridge University Press

TABLE III. Hydrogen bonds in the DFT-optimized crystal structure of tramadol hydrochloride.

D–H···A	D–H (Å)	H···A (Å)	D···A (Å)	D–H···A (Å)	Overlap (*e*)
N21–H45···Cl46	1.051	2.043	3.074	166.3	0.097
O13–H27···Cl46	0.981	2.194	3.172	175.5	0.045
C22–H40···Cl46	1.091	2.554	3.622	166.0	0.013
C20–H38···O11	1.089	2.327	3.362	158.0	0.023
C23–H42···O11	1.088	2.365	3.372	153.2	0.019
C12–H25···O13	1.090	2.603	3.473	136.2	0.016

low-angle peaks, and may indicate subtle changes in the sample during the measurement.

A density functional geometry optimization (fixed experimental unit cell) was carried out using CRYSTAL09 (Dovesi *et al.*, 2005). The basis sets for the H, C, N, and O atoms were those of Gatti *et al.* (1994), and the basis set for Cl was that of Apra *et al.* (1993). The calculation used 8 *k*-points and the B3LYP functional, and took ∼16 days on a 3.0 GHz PC.

III. RESULTS AND DISCUSSION

The refined atom coordinates of tramadol hydrochloride are reported in Table I, and the coordinates from the density functional theory (DFT) optimization in Table II. The root-mean-square (rms) deviation of the non-hydrogen atoms is 0.064 Å, and the maximum deviation is 0.188 Å, at C22 (Figure 3). The excellent agreement between the refined and optimized structures is strong evidence that the structure is correct (van de Streek and Neumann, 2014). After this work was completed, the Bag and Reddy (2014) single-crystal structure appeared. The rms difference between the experimental powder and single-crystal structures is 0.035 Å, and between the DFT and single-crystal structures is 0.053 Å; all three structures are essentially identical. The rms difference between the DFT structure and the cation in VISQAR is 0.139 Å; the cation conformation is very similar in all these structures. The discussion of the geometry uses the DFT-optimized structure. The asymmetric unit (with atom numbering) is illustrated in Figure 4, and the crystal structure is presented in Figure 5.

All of the bond distances, bond angles, and torsion angles fall within the normal ranges indicated by a Mercury Mogul Geometry Check (Macrae *et al.*, 2008). A quantum mechanical conformation examination (DFT/B3LYP/6-31G*/water) using Spartan '14 indicated that the observed conformation is ∼213 kcal mole^{-1} higher in energy than a local minimum, which differs mainly in the orientations of the dimethylammonium and methoxyphenyl portions of the molecule. A molecular mechanics force field sampling of conformational space indicated that the optimized solid-state conformation is 18.9 kcal mole^{-1} higher in energy than the minimum-energy conformation. The energy difference indicates that hydrogen bonds and van der Waals forces contribute significantly to the crystal energy.

The conformations of the dimethylammonium and cyclohexyl portions of the cation in the current structure are similar to those in AYUNUE (Figure 6), but the orientation of the methoxyphenyl groups differ. The energies of these two cations are within 1 kcal mole^{-1} of each other. The tramadol cation seems to have the conformational flexibility to accommodate the needs of its crystallization partners.

Analysis of the contributions to the total crystal energy using the Forcite module of Materials Studio (Accelrys, 2013) suggests that the intramolecular deformation energy is dominated by bond and angle distortion terms. The intermolecular energy is dominated by electrostatic contributions, which in this force-field-based analysis include hydrogen bonds, although van der Waals repulsion is also significant.

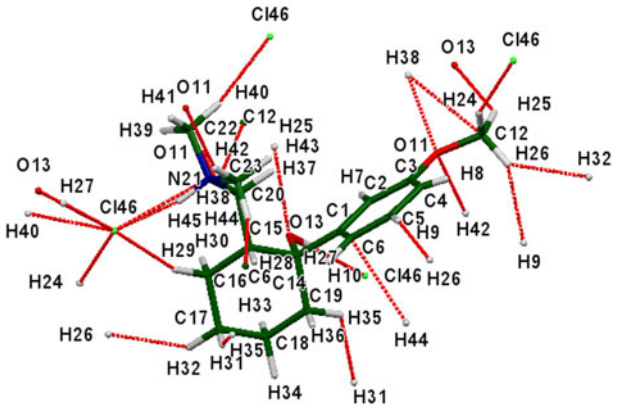


Figure 7. (Color online) Tramadol hydrochloride, showing both the hydrogen bonds and the close intermolecular contacts, as defined by Mercury. All of the C–H···Cl and C–H···O hydrogen bonds are included among the close contacts.

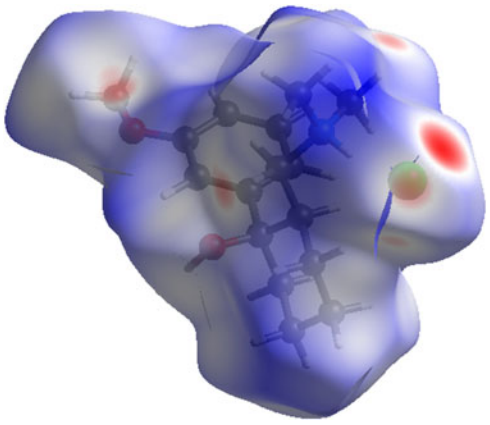


Figure 8. (Color online) The Hirshfeld surface of tramadol hydrochloride. Intermolecular contacts longer than the sums of the van der Waals radii are colored blue, and contacts shorter than the sums of the radii are colored red. Contacts equal to the sums of radii are white.

https://doi.org/10.1017/S088571561500041X Published online by Cambridge University Press

The hydrogen bonds are better analyzed using the results of the DFT calculation.

There are both N21–H45···Cl46 and O13–H27···Cl46 hydrogen bonds (Table III), which form a zigzag chain with graph set (Etter, 1990; Bernstein *et al.*, 1995; Shields *et al.*, 2000) *C*1,2(8) along the *c*-axis. We use the Mulliken overlap populations to identify real hydrogen bonds among the geometrically plausible interactions. Covalent bonds have positive overlap populations, and ionic and non-bonding interactions have small negative overlap populations. The only other positive (>0.01 *e*) overlap populations correspond to reasonable hydrogen bonds. We have examined more sophisticated methods of analyzing the electron density [such as Bader analysis (Bader, 1990)], but they do not change the conclusion about whether a potential hydrogen bond is real. The chloride also acts as an acceptor in a C22–H46···Cl46 hydrogen bond (Figure 7). The ether oxygen O11 participates in two C–H···O hydrogen bonds, and the hydroxyl oxygen O13 participates in a single C–H···O hydrogen bond. Although weak, these C–H donor hydrogen bonds probably contribute significantly to the crystal energy.

The volume enclosed by the Hirshfeld surface (Figure 8; Hirshfeld, 1977; McKinnon *et al.*, 2004; Spackman and Jayatilaka, 2009; Wolff *et al.*, 2012) is 417.08 Å^3, 98.4% of the one-fourth of the unit-cell volume. The molecules are thus not tightly packed. The only significant close contacts (red in Figure 7) involve the hydrogen bonds.

The Bravais–Friedel–Donnay–Harker (Bravais, 1866; Friedel, 1907; Donnay and Harker, 1937) morphology suggests that we might expect a blocky morphology for tramadol hydrochloride, with {010} as the principal faces. A second-order spherical harmonic preferred orientation model was included in the refinement; the texture index was only 1.007, indicating that preferred orientation was not significant in this rotated capillary specimen. The powder pattern of tramadol hydrochloride has been submitted to ICDD for inclusion in the PDF.

SUPPLEMENTARY MATERIALS AND METHODS

The supplementary material for this article can be found at http://www.journals.cambridge.org/PDJ

ACKNOWLEDGMENTS

Use of the Advanced Photon Source at Argonne National Laboratory was supported by the U. S. Department of Energy, Office of Science, Office of Basic Energy Sciences, under Contract No. DE-AC02-06CH11357. This work was partially supported by the International Centre for Diffraction Data. We thank Lynn Ribaud for his assistance in data collection.

Accelrys (**2013**). *Materials Studio 7.0* (Accelrys Software Inc., San Diego, CA).

Allen, F. H. (**2002**). "The Cambridge Structural Database: a quarter of a million crystal structures and rising," Acta Crystallogr. B: Struct. Sci. **58**, 380–388.

Apra, E., Causa, M., Prencipe, M., Dovesi, R., and Saunders, V. R. (**1993**). "On the structural properties of NaCl: an ab initio study of the B1–B2 phase transition," J. Phys.: Condens. Matter **5**(18), 2969–2976.

Bader, R. F. W. (**1990**). *Atoms in Molecules – A Quantum Theory* (Oxford University Press, New York).

Bag, P. P. and Reddy, C. M. (**2014**). "Tramadol hydrochloride and its acetonitrile solvate: crystal structure analysis and thermal studies," Proc. Natl. Acad. Sci. India A **84**(2), 235–242.

Bernstein, J., Davis, R. E., Shimoni, L., and Chang, N. L. (**1995**). "Patterns in hydrogen bonding: functionality and graph set analysis in crystals," Angew. Chem. Int. Ed. Engl., **34**(15), 1555–1573.

Boumendjel, A., Taïwe, G. S., Bum, E. N., Chabrol, T., Beney, C., Sinniger, V., Haudecoeur, R., Marcourt, L., Challal, S., Queiroz, E. F., Souard, F., Le Borgne, M., Lomberget, T., Depaulis, A., Lavaud, C., Robins, R., Wolfender, J.-L., Bonaz, B., and De Waard, M. (**2013**). "Occurrence of the synthetic analgesic tramadol in an African Medicinal Plant," Angew. Chem. Int. Ed. Engl. **52**, 11780–11784; CSD Refcode VISQAR.

Bravais, A. (**1866**). *Etudes Cristallographiques* (Gauthier Villars, Paris).

Brayfield, A. (**2013**). "Tramadol hydrochloride" in *Martindale: The Complete Drug Reference* (Pharmaceutical Press, London).

Bruno, I. J., Cole, J. C., Kessler, M., Luo, J., Motherwell, W. D. S., Purkis, L. H., Smith, B. R., Taylor, R., Cooper, R. I., Harris, S. E., and Orpen, A. G. (**2004**). "Retrieval of crystallographically-derived molecular geometry information," J. Chem. Inf. Sci. **44**, 2133–2144.

Donnay, J. D. H. and Harker, D. (**1937**). "A new law of crystal morphology extending the law of Bravais," Amer. Mineral. **22**, 446–467.

Dovesi, R., Orlando, R., Civalleri, B., Roetti, C., Saunders, V. R., and Zicovich-Wilson, C. M. (**2005**). "CRYSTAL: a computational tool for the *ab initio* study of the electronic properties of crystals," Z. Kristallogr. **220**, 571–573.

Etter, M. C. (**1990**). "Encoding and decoding hydrogen-bond patterns of organic compounds," Acc. Chem. Res. **23**(4), 120–126.

Favre-Nicolin, V. and Černý, R. (**2002**). "FOX, Free Objects for crystallography: a modular approach to ab initio structure determination from powder diffraction," J. Appl. Crystallogr. **35**, 734–743.

Finger, L. W., Cox, D. E., and Jephcoat, A. P. (**1994**). "A correction for powder diffraction peak asymmetry due to axial divergence," J. Appl. Crystallogr. **27**(6), 892–900.

Friedel, G. (**1907**). "Etudes sur la loi de Bravais," Bull. Soc. Fr. Mineral. **30**, 326–455.

Gatti, C., Saunders, V. R., and Roetti, C. (**1994**). "Crystal-field effects on the topological properties of the electron-density in molecular crystals - the case of urea," J. Chem. Phys. **101**, 10686–10696.

Hirshfeld, F. L. (**1977**). "Bonded-atom fragments for describing molecular charge densities," Theor. Chim. Acta **44**, 129–138.

ICDD (**2014**), PDF-4+ 2014 (Database). International Centre for Diffraction Data, edited by Dr. Soorya Kabekkodu (Newtown Square, PA, USA).

Larson, A. C. and Von Dreele, R. B. (**2004**). "General structure analysis system, (GSAS)", Los Alamos National Laboratory Report LAUR 86-784.

Lee, P. L., Shu, D., Ramanathan, M., Preissner, C., Wang, J., Beno, M. A., Von Dreele, R. B., Ribaud, L., Kurtz, C., Antao, S. M., Jiao, X., and Toby, B. H. (**2008**). "A twelve-analyzer detector system for high-resolution powder diffraction," J. Synchrotron Radiat. **15**(5), 427–432.

Macrae, C. F., Bruno, I. J., Chisholm, J. A., Edgington, P. R., McCabe, P., Pidcock, E., Rodriguez-Monge, L., Taylor, R., van de Streek, J., and Wood, P. A. (**2008**). "Mercury CSD 2.0 – new features for the visualization and investigation of crystal structures," J. Appl. Crystallogr. **41**, 466–470.

McKinnon, J. J., Spackman, M. A., and Mitchell, A. S. (**2004**). "Novel tools for visualizing and exploring intermolecular interactions in molecular crystals," Acta Crystallogr. B **60**, 627–668.

MDI (**2014**). *Jade 9.5* (Materials Data. Inc., Livermore, CA).

O'Boyle, N. M., Banck, M., James, C. A., Morley, C., Vandermeersch, and Hutchison, G. R. (**2011**). "Open Babel: an open chemical toolbox," J. Chem. Inf. **3**, 33.

Shields, G. P., Raithby, P. R., Allen, F. H., and Motherwell, W. S. (**2000**). "The assignment and validation of metal oxidation states in the Cambridge Structural Database," Acta Crystallogr. B: Struct. Sci. **56**(3), 455–465.

Siddaraju, B. P., Jasinski, J. P., Golen, J. A., Yathirajan, H. S., and Raju, C. R. (**2011**). "Tramadol hydrochloride-benzoic acid (1/1)," Acta Crystallogr. E **67**, o2351–o2351.

Spackman, M. A. and Jayatilaka, D. (**2009**). "Hirshfeld surface analysis," Crystallogr. Eng. Commun. **11**, 19–32.

Stephens, P. W. (**1999**). "Phenomenological model of anisotropic peak broadening in powder diffraction," J. Appl. Crystallogr. **32**, 281–289.

https://doi.org/10.1017/S088571561500041X Published online by Cambridge University Press

Sykes, R. A., McCabe, P., Allen, F. H., Battle, G. M., Bruno, I. J., and Wood, P. A. (**2011**). "New software for statistical analysis of Cambridge Structural Database data," J. Appl. Crystallogr. **44**, 882–886.

Thompson, P., Cox, D. E., and Hastings, J. B. (**1987**). "Rietveld refinement of Debye–Scherrer synchrotron X-ray data from Al_2O_3," J. Appl. Crystallogr. **20**(2), 79–83.

van de Streek, J. and Neumann, M. A. (**2014**). "Validation of molecular crystal structures from powder diffraction data with dispersion-corrected density functional theory (DFT-D)," Acta Crystallogr. B: Struct. Sci. **70** (6), 1020–1032.

Wang, J., Toby, B. H., Lee, P. L., Ribaud, L., Antao, S. M., Kurtz, C., Ramanathan, M., Von Dreele, R. B., and Beno, M. A. (**2008**). "A dedicated powder diffraction beamline at the Advanced Photon Source: commissioning and early operational results," Rev. Sci. Instrum. **79**, 085105.

Wavefunction, Inc. (**2013**). Spartan '14 Version 1.1.0, Wavefunction Inc., 18401 Von Karman Ave., Suite 370, Irvine CA 92612.

Wolff, S. K., Grimwood, D. J., McKinnon, J. J., Turner, M. J., Jayatilaka, D., and Spackman, M. A. (**2012**). CrystalExplorer *Version 3.1*, University of Western Australia.

https://doi.org/10.1017/S088571561500041X Published online by Cambridge University Press